

Cloud Effects on Photovoltaic Power Forecasting: Initial Analysis of a Single Power Plant Based on Satellite Images and Weather Forecasts

Franko Pandžić¹[0000-0002-3153-2419], Ivan Sudić¹[0000-0002-5703-0513], Tomislav Capuder¹[0000-0002-7657-150X] and Amalija Božiček¹[0000-0003-0331-2707]

¹ Faculty of Electrical Engineering and Computing, University of Zagreb, Croatia

Abstract. Solar power is becoming increasingly important as a source of renewable energy, and photovoltaic (PV) technology has become the key method of harnessing solar energy. Unlike conventional power plants, scheduling PV power production is not possible as it relies on the unpredictable nature of sunlight and local weather conditions. It is why accurate forecasts of power production are crucial for ensuring a stable and reliable supply of electricity. This study is an initial analysis of the effect of local cloud cover on solar production forecasting for Vis power plant. It was shown that even a crude representation of cloud mask images from EUMETSAT can greatly improve production forecasting in a best-case scenario. The model that integrated both solar irradiance and cloud images exhibited superior performance (up to 24 %) compared to the model that solely relied on solar irradiance in the one-hour ahead forecast. These results show great promise in further expanding this research with more advanced algorithms and EUMETSAT products.

Keywords: satellite imagery, solar energy, power plant, forecasting

1 Introduction

The growing demand for clean and sustainable energy sources has accelerated the adoption of renewable energy systems. Among these systems, photovoltaic (PV) technology has gained significant popularity due to its cost-effectiveness and environmental benefits. However, PV systems' performance is subject to weather conditions, making it challenging to accurately forecast their power output. The ability to forecast PV production is crucial for optimal grid integration, efficient energy management, and trading activities. Accurate forecasting also helps to minimize the uncertainty associated with renewable energy production, reducing operational risks and costs.

This paper presents a study on PV production forecasting for a single solar power plant, with a goal to explore the effect of local cloud cover through satellite imagery on the plants' production. The study's primary motivation is to gain insights in data most important for accurate production forecasting along with validating sources of data. The authors distinguish the following papers of importance: Benavides Cesar et al. [1], Hong et al. [2] and Yang et al [3] provide extensive research foundation as

review papers regarding solar forecasting and forecasting energy quantities in general. Qin et al. [4] focus on enhancing PV output forecast by integrating satellite and ground data. They capture cloud motion patterns which they use to forecast PV output forecasts. Holland et al. [5] go a step further and incorporate numerical weather models along with satellite images and ground measurements for large power plants (>500 MW). Contrarily, this study focuses on a 3.5 MW power plant which can pose an issue if following the aforementioned paper. Yu et al. [6] focus on PV forecasting using cloud images as well; first they forecast the amount of cloud coverage and consequently PV output using a convoluted LSTM. Son et al. [7] devise a solution without forecasts of solar irradiance, using only cloud cover images for ultra-short-term and short-term PV forecasting. These papers give foundation for the inclusion of satellite images in order to enhance PV output forecasting, but they mostly use sources of satellite data which may not be easily accessible. Consequently, the authors believe that the source of cloud satellite images in this study is a possible solution to that issue.

The findings of this study have practical implications for any operator in charge of a solar power plant enabling them to make informed decisions based on accurate PV production forecasts generated with the help of satellite images.

1.1 Showcase – Vis solar power plant

For this paper, the showcased power plant is the solar power plant of island Vis, Croatia. HEP Group, which is the national energy company of Croatia, constructed the Vis solar power plant in 2020. with an investment of 31 million kunas (approx. 4.1 million euros), leading to the successful establishment of the plant. The design and construction were done by Končar – Power Plant and Electric Traction Engineering Inc. At the time of its commissioning, SE Vis (from Croatian: *Sunčana elektrana*) was the highest-capacity solar production sight in Croatia with the capacity of 3.5 MW. SE Vis contains 11200 modules with an individual power of 340 Wpp. Next to SE Vis, a battery tank with a power of 1 MW and a capacity of 1.44 MWh is installed, the first of its size in Croatia at that time. The battery tank is used to provide power system balancing services and for the purpose of preserving the stability of the network on the island, capable of powering up to 1600 households. The total area on which the facility is located is 5.5 ha (13.6 acres) [8]. The coordinates of the power plant are 16.141 longitude and 43.038 latitude, and its layout can be seen using Google Maps.

2 Data

Available data includes production measurements from Vis solar power plant, weather forecasts for the location of the plant obtained by Weather Research & Forecasting Model (WRF) [9] and EUMETSAT satellite imagery [10].

2.1 SE Vis historical production

Production measurements of SE Vis are available in 15 minute intervals from 03.09.2020. 02:00 UTC until 14.07.2022. 06:45 UTC (almost 2 years of data). Fig. 1. shows the **mean** and **median** photovoltaic production for SE Vis for the aforementioned period. The median peak production (1.96 MW) is higher than the mean peak production (1.67 MW). This discrepancy implies that there are non-insignificant number of days when the production levels, which are expected to be at their highest, are impeded by factors such as local cloud cover.

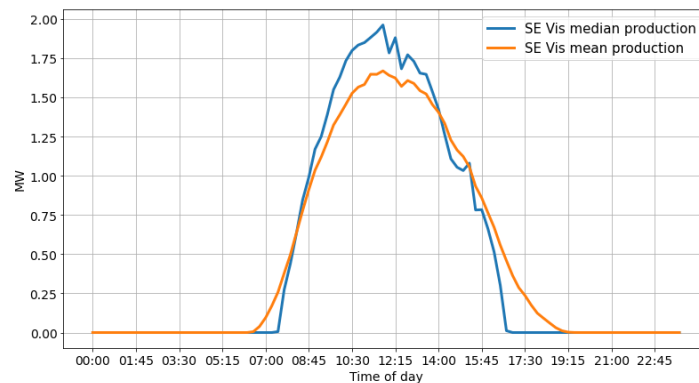


Fig. 1. SE Vis **mean** and **median** production through time of day

2.2 WRF Forecasts

WRF forecasts are available every 6 hours for the next 72 hours starting from midnight UTC every day for SE Vis location. Specifically, new forecasts are available at 00:00, 06:00, 12:00 and 18:00 UTC every day. Forecasts of 7 meteorological phenomena are available to the authors:




- Wind speed (m/s)
- Wind direction (°)
- Composite reflectivity (dBZ)
- Air temperature (°C)
- Air pressure at sea level (hPa)
- Relative humidity (%)
- Solar irradiance (W/m²)

2.3 EUMETSAT satellite imagery

The *European Organisation for the Exploitation of Meteorological Satellites* (EUMETSAT) was created through an international convention agreed by a current total of 30 European Member States. Their primary goal is to establish, maintain and utilize the European system of meteorological satellites. They offer multiple weather products such as images of cloud masks, microphysics models etc. For the purpose of

this paper, the simplest product will be investigated – *clm* (Cloud Mask) which is obtained via Meteosat Second Generation (MSG) Geostationary (GEO) satellites. These satellites use an optical SEVIRI sensor to obtain cloud mask images.

clm products categorize surfaces into four classes, one of which is *not processed surfaces*, leaving three classes that offer valuable information. Table 1. explains the three classes and their representation on an image.

Pixel Color	Description
	Clear sky over land
	Cloud
	Clear sky over water

Images were retrieved via EUMETSAT API for latitudes between 41° and 45° and longitudes between 14° and 18° . In other words, the images cover an area of approximately $444.4 \text{ km} * 444.4 \text{ km}$. This area was chosen to have the island of Vis in the middle and have enough of the surrounding area for further research (forecasting cloud movement etc.). *clm* image resolution is approximately 2.2 km (one pixel covers an area of approximately $2.2 \text{ km} * 2.2 \text{ km}$). Fig. 2. shows examples of *clm* images. The red ellipsoid highlights the island of Vis. Fig. 2. (a) features a clear day without much cloud coverage (few white pixels) while Fig. 2. (b) shows a cloudy day over the Mediterranean. Although *clm* images are available in 5-min intervals, they were retrieved at 15-min intervals for times corresponding to those of SE Vis production measurements for easier data manipulation and analysis.

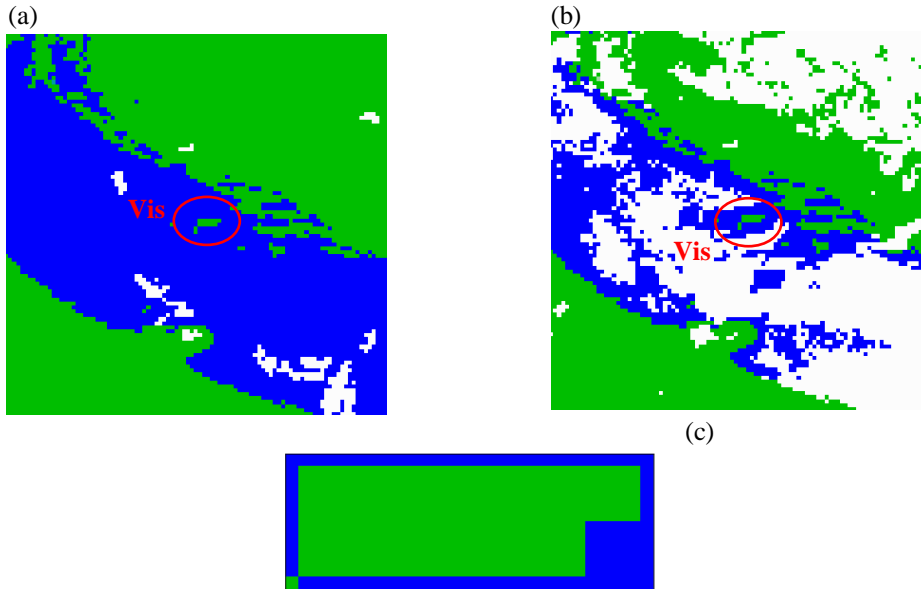


Fig. 2. (a) *clm* image for 05.09.2020. 08:15 UTC – clear day (b) *clm* image for 14.09.2020. 05:00 UTC – cloudy day (c) key pixels for determining cloud coverage

3 Analysis

To represent satellite images as a time series variable, a simple transformation was done. Only pixels part of the bounding box encompassing the entirety of the island of Vis were taken into consideration (Fig. 2. (c)). Information from images was converted to cloud coverage (cc). For every time step t (image), the following was calculated:

$$cc_t = \frac{P_c}{P_{tot}} \quad (1)$$

P_c is the number of cloud pixels and P_{tot} is the number of total pixels. If relied solely on the global Pearson's correlation coefficient (singular value for the entire time series), which stands at $\rho = -0.28$, the relationship between cloud coverage and production would be considered weak. Fig. 3. displays the correlation coefficient calculated for each 15-minute interval of the day (00:00-23:45). The results indicate that during the night hours when there is no production, the correlation is weak. In other words, the night hours reduce the global correlation significantly. On the other hand, for hours when there is irradiance and thus production, the dependence between cloud coverage and production is relatively strong ($\rho \sim -0.7$).

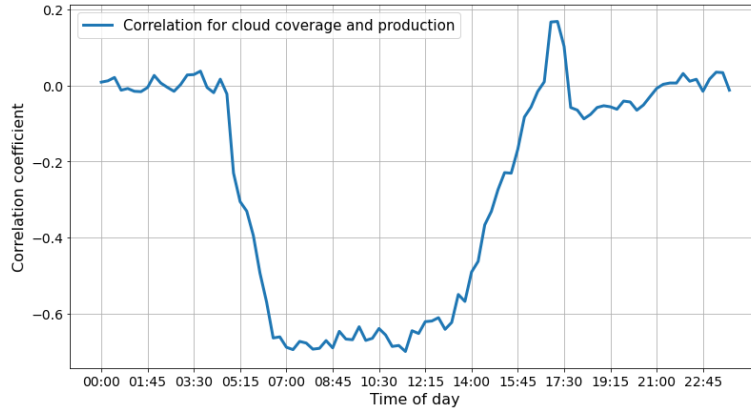


Fig. 3. Pearson correlation coefficient for cloud coverage and SE Vis production

To isolate the impact of cloud coverage, only the most significant WRF forecast will be utilized hereafter. To effectively merge the 15-minute interval production data with the forecast data, which is recorded in hourly intervals, the production data needed to be averaged over hourly intervals. Fig. 4. shows the correlation between all available meteorological parameters and SE Vis production. As expected, forecasts of solar irradiance have the highest positive linear dependence with production ($\rho = 0.89$). As the goal of this paper is to explore the effect of local clouds on production forecasting,

and not specifically the optimal production forecast, other meteorological phenomena are disregarded. If developing and optimal forecast of production, exploring other meteorological variables would be necessary. In the next subsection simple regression models are used to determine the effect of cloud coverage on production forecasting.

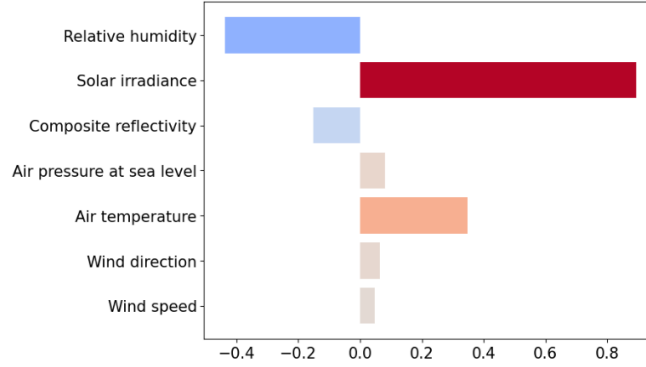


Fig. 4. Bar plot of correlations of meteorological parameter forecasts SE Vis production

4 Model Training and results

To determine the impact of cloud coverage acquired from cloud mask satellite images on power production, two simple regression models based on the same architecture were trained. One is a *base* model as it only uses solar irradiance forecasts as inputs while *cloud* model uses cloud coverage and irradiance forecasts as inputs. Comparing errors of both models can clearly show if the inclusion of cloud coverage helps improve production forecasting.

Ridge regression with the same level of regularization was used for both *base* and *cloud* models. Samples $(input, target)$ for every timestep t were created as:

$$\begin{aligned} sample_t^{base} &= (irradiance_t, production_t) \\ sample_t^{cloud} &= ([irradiance_t, cloud\ coverage_t], production_t) \end{aligned} \quad (2)$$

Only the most recent WRF irradiance forecasts were considered. 70 % samples were used for training, 15 % for validation and the remaining 15 % for testing. Models were trained, validated, and tested only for hours of the day for which production was measurable (night hours were disregarded). Fig. 5. shows the mean squared error (MSE) for *base* and *cloud* models for each hour of the day of the test set. Scaled average production is also shown as the errors for peak production hours (7th to 14th hour UTC) are more important than the ones which have less production. *cloud* model outperforms the *base* model for almost all hours based on MSE.

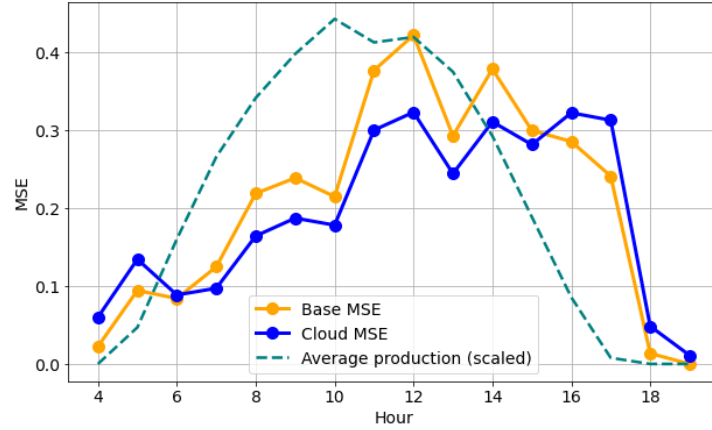


Fig. 5. MSE (*base* and *cloud*) for each hour of the day with **scaled average production** for reference of error significance

cloud model performs even better when observing only peak production hours, with the 12th hour exhibiting the largest MSE discrepancy (0.322 vs 0.421, 24 % difference). Table 2. condenses information from Fig. 5. and shows the improvements made using *clm* images in one-hour ahead forecast production.

Table 2. Average MSE for total and peak hours

	MSE (total)	MSE (peak hours)
<i>base</i>	0.206	0.283
<i>cloud</i>	0.191	0.225
improvement	7.3 %	20.5 %

5 Conclusion and future work

It was shown in this paper that the simple inclusion of EUMETSAT satellite images, specifically the cloud mask product, can greatly improve one-hour ahead production forecasting. The findings of this research can be implemented by any solar power plant operator to optimize management. Still, it needs to be mentioned that satellite images are taken in real-time and not available in advance (an hour before). As this paper is considered as an initial case study, cloud images were regarded as perfect forecasts. Consequently, results of this work can be considered as best-case scenario (having perfect forecast of cloud coverage). The authors recognize three important factors that can be improved upon and potentially greatly improve one-hour ahead production forecasts:

- (i) Image representation as a single value to models resulted in information loss. To improve upon this, more advanced transformations need to be explored.

- (ii) A simple linear architecture was used to investigate the effect of cloud information on production forecasting. More advanced architectures need to be explored. Namely, deep neural networks which can extract key information from original images directly.
- (iii) *clm* product does not differentiate between clouds. More advanced EUMETSAT products can address this limitation. Namely, a microphysics product (*mphys*) [11] categorizes clouds into five possible classes which extends available information.

To create a viable model, cloud forecasts must be developed. This can be done using advanced algorithms such as deep neural networks using consequent images or with motion estimation algorithms. However, the next step before cloud forecasting, would be determining the most adequate EUMETSAT product (possibly *mphys*) for tackling this issue.

References

1. Benavides Cesar, L., Amaro e Silva, R., Manso Callejo, M.Á., Cira, C.I., Review on spatio-temporal solar forecasting methods driven by in situ measurements or their combination with satellite and numerical weather prediction (NWP) estimates. *Energies*.
2. Hong, T., Pinson, P., Wang, Y., Weron, R., Yang, D., and Zareipour, H., "Energy Forecasting: A Review and Outlook," in *IEEE Open Access Journal of Power and Energy*, vol. 7, (pp. 376-388) (2020)
3. Yang, D., Kleissl, J., Gueymard, C.A., Pedro, H.T., Coimbra, C.F., History and trends in solar irradiance and PV power forecasting: A preliminary assessment and review using text mining. *Solar Energy*. 2018 Jul 1;168:60-101.
4. Qin, J., Jiang, H., Lu, N., Yao, L., & Zhou, C. Enhancing solar PV output forecast by integrating ground and satellite observations with deep learning. *Renewable and Sustainable Energy Reviews*, 167, 112680 (2022).
5. Son, Y., Yoon, Y., Cho, J., & Choi, S. Cloud Cover Forecast Based on Correlation Analysis on Satellite Images for Short-Term Photovoltaic Power Forecasting. *Sustainability*, 14(8), 4427 (2022).
6. EUMETSAT, <https://www.eumetsat.int/>, (accessed 2023/03/14).
7. SEVIRI Day Microphysics RGB Quick Guide, <https://www.eumetsat.int/media/41625>, (accessed 2023/03/14).
8. Holland, N., Pang, X., Herzberg, W., Karalus, S., Bor, J., & Lorenz, E. Solar and PV forecasting for large PV power plants using numerical weather models, satellite data and ground measurements. In 2019 IEEE 46th Photovoltaic Specialists Conference (PVSC) (pp. 1609-1614). IEEE (2019).
9. Skamarock, W. C., Klemp, J. B., Dudhia, J., Gill, D. O., Liu, Z., Berner, J., ... Huang, X. -yu. (2021). A Description of the Advanced Research WRF Model Version 4.3 (No. NCAR/TN-556+STR).
10. Yu, D., Seowoo L., Sangwon L., Wonik C., & Ling L. "Forecasting photovoltaic power generation using satellite images." *Energies* 13, no. 24: 6603 (2020).
11. HEP <https://www.hep.hr/u-rad-pustena-suncana-elektrana-vis-najveca-suncana-elektrana-u-hrvatskoj/3549> (accessed 2023/03/14)

Authors' background

Your Name	Title*	Research Field	Personal website
Franko Pandžić	PhD candidate	Power systems	https://www.fer.unizg.hr/en/franko.pandzic
Ivan Sudić	PhD candidate	Power systems	https://www.fer.unizg.hr/en/ivan.sudic
Tomislav Capuder	Associate professor	Power systems	https://www.fer.unizg.hr/en/tomislav.capuder
Amalija Božiček	PhD candidate	Power systems	https://www.fer.unizg.hr/en/amalija.bozicek

*This form helps us to understand your paper better, **the form itself will not be published.**

*Title can be chosen from: master student, Phd candidate, assistant professor, lecture, senior lecture, associate professor, full professor